Chinese Journal of Aeronautics 24 (2011) 701-708

Contents lists available at ScienceDirect

Chinese Journal of Aeronautics

journal homepage: www.elsevier.com/locate/cja

Preliminary Experimental Investigation on MHD Power Generation Using Seeded Supersonic Argon Flow as Working Fluid

LI Yiwen[a], LI Yinghong[a,*], LU Haoyu[b], ZHU Tao[a], ZHANG Bailing[a], CHEN Feng[a], ZHAO Xiaohu[a]

[a]*Science and Technology on Plasma Dynamics Laboratory, Air Force Engineering University, Xi'an 710038, China*

[b]*School of Astronautics, Beihang University, Beijing 100191, China*

Received 12 December 2010; revised 14 February 2011; accepted 2 June 2011

Abstract

This paper presents a preliminary experimental investigation on magnetohydrodynamic (MHD) power generation using seeded supersonic argon flow as working fluid. Helium and argon are used as driver and driven gas respectively in a shock tunnel. Equilibrium contact surface operating mode is used to obtain high temperature gas, and the conductivity is obtained by adding seed K_2CO_3 powder into the driven section. Under the conditions of nozzle inlet total pressure being 0.32 MPa, total temperature 6 504 K, magnetic field density about 0.5 T and nozzle outlet velocity 1 959 m/s, induction voltage and short-circuit current of the segmentation MHD power generation channel are measured, and the experimental results agree with theoretical calculations; the average conductivity is about 20 S/m calculated from characteristics of voltage and current. When load factor is 0.5, the maximum power density of the MHD power generation channel reaches 4.797 1 MW/m^3, and the maximum enthalpy extraction rate is 0.34%. Finally, the principle and method of indirect testing for gas state parameters are derived and analyzed.

Keywords: magnetohydrodynamic; power generation; conductivity; shock tunnel; supersonic

1. Introduction

Along with the increase of flight Mach number, the combustor inlet temperature increases, and higher temperature causes some problems: one is energy loss due to unequilibrated dissociation; the other is that the fuel added to burner decreases due to temperature limit set by the wall materials and cooling methods, and it causes the unit thrust of the engine to reduce rapidly. A new method is needed to solve this problem when flight speed extends to hypersonic.

In the 1990s, Russian scientists proposed AJAX vehicle concept[1-2], a magnetohydrodynamic (MHD) bypass engine, based on the idea of redistributing energy among various stages of the propulsion system flow train. The system uses an MHD generator to extract a portion of the aerodynamic heating energy from the inlet and an MHD accelerator to reintroduce this power as kinetic energy in the exhaust stream. In this way, the inlet Mach number of the combustor can be limited to a specified value even as the flight Mach number increases. Thus, the fuel and air can be efficiently mixed and burnt within a practical combustor length, and the flight Mach number operating envelope can be extended.

Moreover, when the ramjet is working, it cannot generate electrical energy with traditional methods due to no rotating machinery; so the generated electrical energy by MHD generator could be used to power

*Corresponding author. Tel.: +86-29-84787526.
E-mail address: yinghong_li@126.com
Foundation items: National Natural Science Foundation of China (10972236); The Scientific and Technical Innovation for Postgraduates of Air Force Engineering University (DX2010102)

doi: 10.1016/S1000-9361(11)60082-4

various devices on-board.

The AJAX concept has attracted broad attention from all over the world [3-8], including American researchers. American National Aeronautics and Space Administration (NASA) Glenn research center proposed a concept of MHD energy bypass with a conventional turbojet [9-10], which plans to extend the operating range of turbojet from Mach number 3 to 7.

For the AJAX and MHD combined turbojet engine, the fundamental idea is to use MHD energy conversion processes to extract and bypass a portion of the intake kinetic energy around the burner. In this way, the overall static temperature rise associated with inlet flow deceleration can be actively constrained, and the propulsion system is able to reach a higher freestream Mach number.

In the recent years, thermodynamic analysis for MHD bypass engines has proved that the idea is correct [11-13]. However, due to the multiplicity and complexity of MHD system and restricted by present technology, there still exist many problems to settle, especially for MHD power generation.

In the US Air Force Hypersonic Vehicle Electric Power System (HVEPS) program [14-15], researchers are collaborating on research and development of scramjet driven by MHD power for an advanced high power, airborne electric power system. Initial work under the HVEPS program were directed at engineering evaluations and vehicle integration of different types of MHD power systems, and their preliminary experiments with alkali metal seeded showed that the generated maximum power reached 15 kW. Murray, et al. [16], first succeeds in generating 42 mW electric energy through ionizing the Mach number 3 supersonic flow with nanosecond pulse to achieve conductivity in the flow. Lee and Lu [17-18] has developed numerical simulation on MHD generator. The Institute of Electrical Engineering, Chinese Academy of Sciences conducted open cycle coal MHD power generation experiments in the 1980s, and the K_2CO_3 solution was used in their experiment [19]. In this paper, MHD power generation experiment system is established; helium is used for driver gas and argon is used for driven gas; equilibrium contact surface operating mode is used for getting high temperature gas, and the conductive gas is obtained by adding seed K_2CO_3 powder into the driven section; preliminary experi-mental investigation on MHD power generation is performed.

2. Experimental Principle and Setup

2.1. Principle of MHD power generation

Fig. 1 illustrates the experimental principle of MHD power generation. Its basic principle is also the law of electromagnetic induction. The working medium is conductive supersonic flow, which enters the channel at velocity u, inducing an electric field and producing an electric current in the flow. A part of the kinetic energy of the flow can be converted into electricity, which goes with the slowing down of the flow.

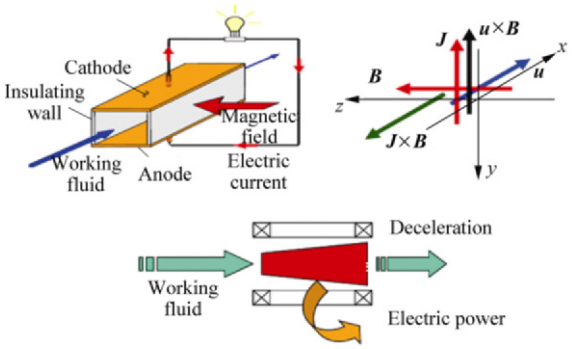

Fig. 1 Principle of MHD power generation.

According to the structure, MHD channel can be divided into four types: continuous faraday generator, segmented faraday generator, Hall generator and diagonal generator. In this paper, the segmented faraday generator is selected in our experimental research for its high efficiency, clear principle and simple structure.

2.2. Shock tube facility

Fig. 2 shows a schematic of the experimental system. It consists of shock tube, nozzle and testing section, vacuum tank, control and measurement system, as well as seeder and magnet.

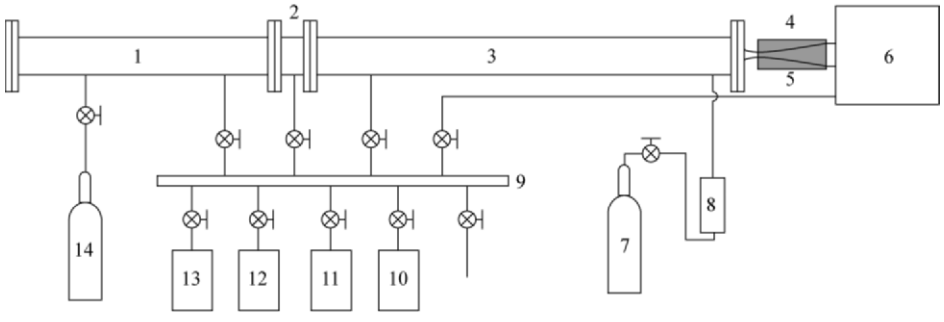

1—Driver section; 2—Buffer; 3—Driven section; 4—Testing section; 5—Magnet;
6—Vacuum tank; 7—Argon; 8—Seeder; 9—Distribution cylinder; 10—Compressor;
11—Vacuum pump; 12—Pressure gauge; 13—Vacuometer; 14—Helium

Fig. 2 Schematic of experimental system.

Physical picture of the experimental system is shown in Fig. 3. Inner dimension of the rectangular tube is 130 mm×80 mm. The driver (high pressure) and driven (low pressure) sections are separated by a double-diaphragm device, which is ruptured by controlling the interspace pressure. The thickness of the diaphragm (polyester film) is 0.1 mm. Working gas of high pressure and high temperature is produced at the outlet of the driven section and flows through the MHD power generation channel to the dump tank, which has sufficient volume to keep backpressure constant.

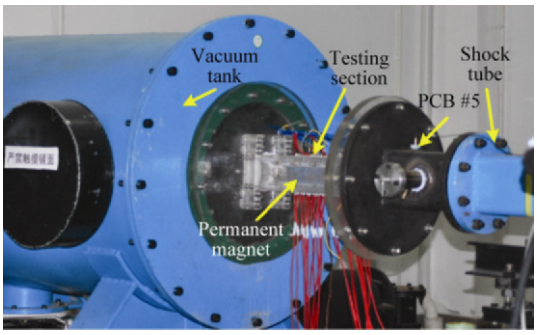

Fig. 3 Physical picture of experimental system.

According to conventional shock relation, the relationship between the tube length and the effective experimental time is shown in Table 1. It is calculated on condition that Ma_s=4.676, where Ma_s is the Mach number of the incidence shock wave. When L_H (the length of high pressure section) is 12 m and L_L (the length of low pressure section) is 2 m, the shock tunnel has the longest experimental time. However, it needs more helium for its longer driver section. Considering the factors of time and cost, the scheme of L_H = 6 m, L_L = 8 m is selected, and its effective experimental time calculated is 9.7 ms.

Table 1 Relationship between tube length and effective experimental time (Ma_s = 4.676)

Length/m	L_H=6 L_L=8	L_H=4 L_L=10	L_H=2 L_L=12	L_H=8 L_L=6	L_H=10 L_L=4	L_H=12 L_L=2
Effective experimental time/ms	9.7	5.9	2.0	13.6	17.4	21.3

2.3. Ionization

In the MHD power generation experiment, the gas must be ionized and have high electrical conductivity in order to attain effective MHD interaction in the generator. In this system, conductivity gas is obtained by added alkali metal material under high temperature (more than 2 500 K) for its low ionization potential. In general, seed of 1%-2% mass flow is required [19].

Fig. 4 shows the schematic of the injection of the powder with argon into the driven section. The seed material, K_2CO_3, is processed to a mean size of 5 μm diameter by a globe mill. A typical seeder operational sequence is as follows: the seeder is placed in the cup on top of a 300-mesh screen before it is closed. After the vacuum is drawn, the argon gas flows through the seed bath whereas the argon seed with K_2CO_3 powder fills up the driven section and acts as the working fluid. In order to make the seeded argon flow into the driven section smoothly, vacuum pumping position is located on the left of the driven section, and the injection position on the right. After filling process is finished and pressure is vacuumized to scheduled value, the experiment is finished by rupturing the film.

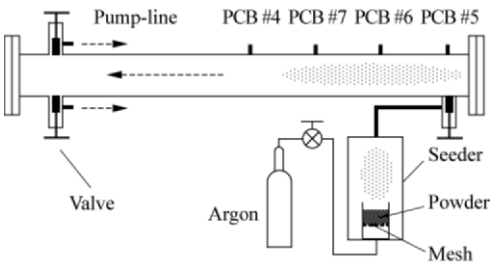

Fig. 4 Schematic of injection of powder with argon into driven section.

2.4. Test section

The test section consists of a supersonic nozzle (*Ma*=2.0), a diffuser and a MHD power generation channel, shown in Fig. 5. The height of the throat is 5.438 mm, the diffuser is 70 mm long and the MHD power generation channel is 116 mm long with a 0.75° divergence angle. The channel width is a constant of 20.0 mm. Magnetic field is applied by Nd-Fe-B rare-earth permanent magnet; the magnetic field strength at the central position is about 0.5 T, and at the end position is about 0.3 T, which is measured by a HT201 Gauss meter. Due to the low magnetic field strength, the Hall parameter is also small in our experimental conditions. The segmented faraday MHD power generation channel is selected for our experiment. It has 10 pairs of electrodes. The channel heights of the first and the tenth electrode pairs are 11.84 mm and 14.66 mm respectively. The electrode pitch is 4.0 mm and its width is 8.0 mm.

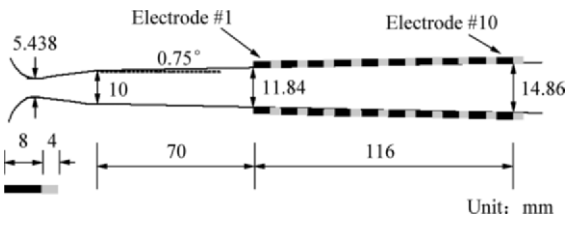

Fig. 5 Schematic of nozzle and test section.

2.5. Diagnostics and data acquisition system

For the measurement of electrical parameters, TekP6139A voltage probe is used for voltage meas-

urement, and TCPA300＋TCP312 current probe is used for current measurement, which are acquired and saved by DPO4104 oscilloscope.

Four quartz crystal PCB pressure transducers are located in the walls of the driven tube as shown in Fig. 4. The farthest transducer downstream is located at the port just upstream of the nozzle entrance (PCB #5), one transducer is adjusted in the pitot tube installed 30 mm downstream the last pair of electrodes (the tenth), and PCB pressure transducer signals are acquired by 8-channels PCI-20612 high speed data acquisition processor. The pressure of driven section is monitored by an absolute pressure transducer.

3. Results and Analysis

3.1. Experimental conditions

Fig. 6 shows the pressure p operation curves of the shock tube. PCB #1 stands for the total pressure of the working section, and PCB #5 the total pressure of area 5 at the end of low pressure section; towards high pressure section there are PCB #6, PCB #7 and PCB #4. From the pressure operation curves the experimental conditions could be acquired.

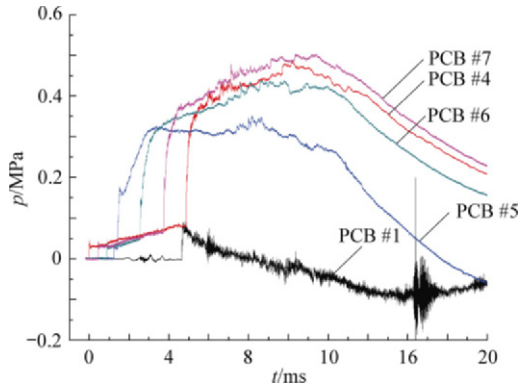

Fig. 6 Pressure operation curves of shock tube.

Because the intensity of shock wave reflecting from the contact surface decreases rapidly, it can be assumed that the compression process after the first interaction between the shock wave and the contact surface is isentropic (the isentropic index is γ), therefore, the equilibrium temperature T_e is

$$\frac{T_e}{T_5}=\left(\frac{p_e}{p_5}\right)^{\frac{\gamma-1}{\gamma}} \tag{1}$$

where p_5 is the actual measurement pressure of area 5, p_e the actual measurement equilibrium pressure, and T_5 is calculated by using conventional shock relation, as shown in Eqs. (2)-(3).

$$T_{51}=\frac{[2(\gamma-1)Ma_s^2-(\gamma-3)][(3\gamma-1)Ma_s^2-2(\gamma-1)]}{(\gamma+1)^2Ma_s^2} \tag{2}$$

$$T_5=T_{51}T_1 \tag{3}$$

And the nozzle outlet density ρ of the Ma=2.0 supersonic flow can be calculated by Eq. (4).

$$\rho=\rho_e\left(1+\frac{\gamma-1}{2}Ma^2\right)^{-\frac{1}{\gamma-1}} \tag{4}$$

where ρ_e is decided by the state formula of ideal gas:

$$\rho_e=\frac{p_e}{R_aT_e} \tag{5}$$

where R_a is gas constant of argon.

The experimental conditions are listed in Table 2.

Table 2 Experimental conditions

Parameter	Value
High pressure section p_4/MPa	0.7
Low pressure section p_1/Pa	1 000
Actual measurement incident shock wave Ma_s	4.676
Actual measurement equilibrium pressure p_e/MPa	0.32
Equilibrium temperature T_e/K	6 504
Nozzle outlet static temperature T/K	2 732
Nozzle outlet velocity u/(m·s^{-1})	1 959
Nozzle outlet density ρ/(kg·m^{-3})	0.067 4

3.2. Experimental results

Fig. 7 shows the voltages U of electrodes #1, #5, #10 under the conditions listed in Table 2. The voltages are measured through open-circuit, and Fig. 8 is the schematic of measuring method.

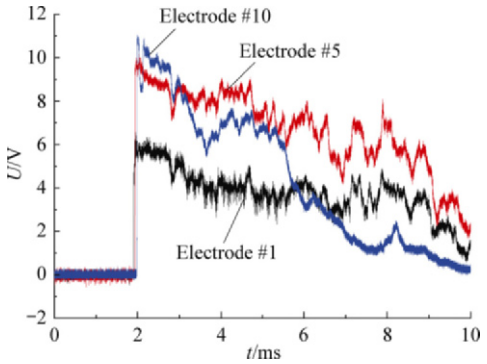

Fig. 7 Electric voltage signals on electrodes #1, #5 and #10.

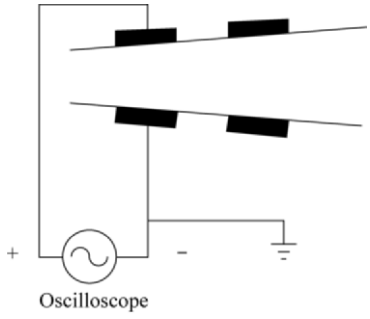

Fig. 8 Schematic of open-circuit voltage measurement.

According to the law of electromagnetic induction, when the velocity of the conductor is u, the induction parameter is B and the load factor is K, the electrical field strength E is

$$E = KuB \tag{6}$$

where K is the ratio between the load resistance of generator R and total resistance (R and intrinsic resistance R_i), and $K<1$.

$$K = \frac{R}{R+R_i} = \frac{E}{uB} \tag{7}$$

When the measurement is performed in the open-circuit, the load factor K=1. The voltages acquired from Fig. 7 are identical with the theoretical calculation of Eq. (6). The voltage at electrode #1 is 6.3 V, the magnetic induction parameter 0.3 T, the voltage at electrode #5 11.6 V, and the magnetic induction parameter 0.5 T. For the electrode #10, the voltage decreases. Because the main cause is that with the increase of shock tunnel running time, the pressure and temperature at area 5 decrease, which leads to the decrease of the velocity at nozzle exit. Besides, the voltage at electrode #10 is not much bigger than that at electrode #5. However, with the running time increasing, the voltage decreases sharply. It is because that the flow is speeding up in the expanding tunnel, which decreases the temperature and conductivity. Besides, the boundary layer becomes thicker, which will enlarge the voltage drop at the electrode. Both of the factors above contribute to the decrease of the voltage.

Fig. 9 shows the short-circuit current I at electrode #6, while Fig. 10 is the schematic of its measuring method. Since electrode #5 and electrode #6 are close enough, their voltage and current characteristics could be taken as the same. Under the conditions of high temperature, there would be some cupric oxide on the surface of electrode, and the resistance is very big, which severely weakens the electric conduction of electrode. Experiments show that it is very difficult to acquire the short-circuit current. Actually, due to the decline in performance caused by electrode oxidation，the measured current is smaller than the real current.

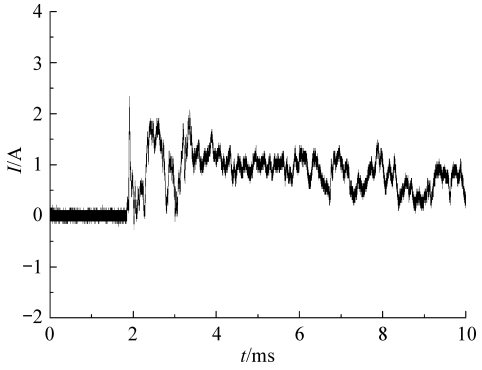

Fig. 9 Current signal on electrode #6.

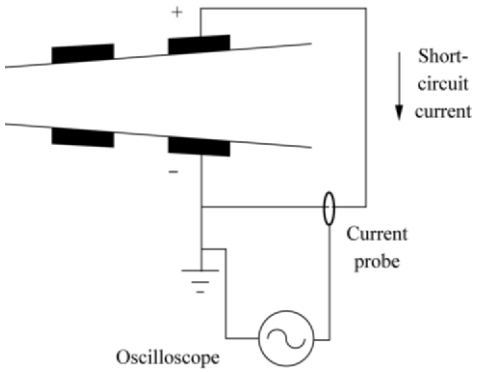

Fig. 10 Schematic of short-circuit current measurement.

The current density j created by induced electromotive force is

$$j = \sigma(uB - E) = (1-K)\sigma uB \tag{8}$$

The conductivity σ can be calculated with the voltage and current profile, and the power density P is described as

$$P = jE = K(1-K)\sigma u^2 B^2 \tag{9}$$

Fig. 11 shows the profile of conductivity from the voltage and current of electrode #5 and electrode #6. Because the voltage and current is acquired from different electrodes, the conductivity is only an equivalent value, which is about 20 S/m. Using the conductivity, velocity, magnetic field strength and other parameters, the relationship between MHD power density and load factor can be calculated: when the load factor is 0.5, the maximum power density is 4.797 1 MW/m^3.

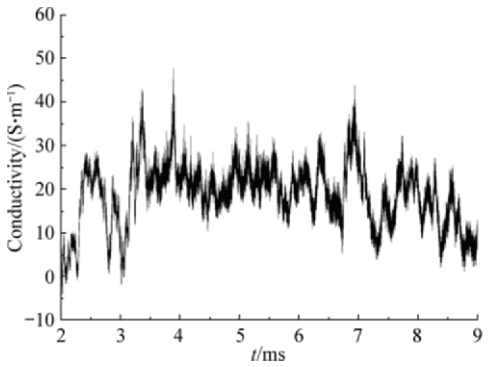

Fig. 11 Conductivity of supersonic flow calculated from voltage and current of electrode #5 and electrode #6.

3.3. Analysis

The enthalpy extraction rate can be used to describe the efficiency of MHD generating tunnel as

$$\eta_{N(g)} = \frac{K(1-K)\sigma u^2 B^2 V}{m_a c_p T_e} \tag{10}$$

where V is the volume of MHD power generation channel, m_a the mass flow (which is 0.021 8 kg/s in

this paper), c_p the heat capacity at a constant pressure. Under the conditions discussed in this paper, the enthalpy extraction rate $\eta_{N(g)}$ is 0.34%. It can be seen from Eq. (10) that the increase of conductivity and magnetic field strength can help to raise the enthalpy extraction rate in the MHD generation channels.

Owing to a low magnetic field strength in this experiment, MHD power generation can hardly change the parameters of flow after the working section. It is, therefore, hardly possible to analyze them through experimental measurement.

From the analysis mentioned above, we can conclude that the electrical conductivity is a critical parameter, for it determines the minimum magnetic field strength required for achieving meaningful levels of MHD interaction. For example, lower conductivity implies the need for larger, heavier and more power-hungry electromagnets. In general, the manifestation of significant MHD effects requires a MHD interaction parameter Q which is defined as the ratio of MHD forces to the inertial forces in the flow and its expression is as follows:

$$Q = \frac{\sigma B^2 L}{\rho u} \tag{11}$$

where L is the characteristic length.

According to Kuranov's research [6], to noticeably improve scramjet performance, it is necessary to ensure that MHD interaction parameter $Q > 0.1$. However, in this experiment, Q is calculated to be about 0.006 6, which is less than needed.

The electrical conductivity is mainly caused by the electron, which can be described as

$$\sigma = \frac{n_e e^2 \tau}{m_e} = \frac{n_e e^2}{m_e n Q_{en} C_e} \tag{12}$$

where e is the electron charge, m_e the electron mass, n the atomic or molecular density, τ the time between twice collisions, n_e the electron density, Q_{en} the electron collision cross section, and C_e the average thermal velocity of electron.

The Hall parameter is described as

$$\beta = \omega\tau \tag{13}$$

where ω is the cyclotron frequency described by electron and ion.

$$\omega_e = \frac{eB}{m_e} \tag{14}$$

$$\omega_i = \frac{eB}{m_i} \tag{15}$$

$$\tau_e = \frac{1}{nQ_{en}C_e} \tag{16}$$

$$\tau_i = \frac{1}{nQ_{in}C_i} \tag{17}$$

where m_i is the ion mass, Q_{in} the ion collision cross section, C_i the average thermal velocity of ion, and C_e and C_i are described as

$$C_e = \sqrt{\frac{8kT_e}{\pi m_e}} \tag{18}$$

$$C_i = \sqrt{\frac{8kT_i}{\pi m_i}} \tag{19}$$

Therefore, the electron Hall parameter is

$$\beta_e = \frac{\sigma B}{e n_e} \tag{20}$$

and

$$\frac{\omega_e \tau_e}{\omega_i \tau_i} = \frac{Q_{in}}{Q_{en}} \sqrt{\frac{m_i T_i}{m_e T_e}} \tag{21}$$

Based on the assumption that Q_{in} has the same magnitude with Q_{en}, and so do T_i and T_e, then the ratio of β_e to β_i becomes [19]

$$\frac{\beta_e}{\beta_i} = \frac{\omega_e \tau_e}{\omega_i \tau_i} \approx \sqrt{\frac{m_i}{m_e}} \tag{22}$$

The electron density n_e is $2.025\ 5\times10^{20}/\mathrm{m}^3$ according to Saha equation:

$$\frac{n_e n_i}{n_a} = \frac{(2\pi m_e kT)^{\frac{3}{2}} n_e n_i}{h^3} \cdot \frac{2g_i}{g_a} \exp\left(-\frac{e\varepsilon_i}{kT}\right) \tag{23}$$

where n_i, n_a are the ion and seed atom density, k is the Boltzmann constant, h the Planck constant, ε_i the ionization potential, g_i the percent of ion ground state, g_a the percent of atom ground state, and $2g_i/g_a \approx 1$ for alkali.

The calculated electron Hall parameter β_e in the MHD interaction region is 0.308 6, and the ion Hall parameter β_i is 0.001 2, which is much smaller than β_e.

If the ion-slip is considered, the electric conductivity Σ and Hall parameter Ω are changed to be [19]:

$$\Sigma = \frac{\sigma}{1 + \omega_e \tau_e \omega_i \tau_i} \tag{24}$$

$$\Omega = \frac{\omega_e \tau_e}{1 + \omega_e \tau_e \omega_i \tau_i} \tag{25}$$

When the magnetic field strength is 0.5 T, the calculated Σ is 19.992 9 S/m, and Ω is 0.308 5, which indicates that the ion-slip can be ignored. However, if the magnetic field strength increases to 3 T or 10 T, the electric conductivity Σ and hall parameter Ω will be changed strongly when the gas electrical conductivity σ keeping 20 S/m (see Table 3).

Table 3 Calculated parameters

B/T	σ/(S•m^{-1})	β_e	Σ/(S•m^{-1})	Ω
0.5	20	0.308 6	19.992 9	0.308 5
3	20	1.851 4	19.746 5	1.827 9
10	20	6.171 2	17.503 1	5.400 8

Besides, in order to obtain the gas state parameters of inlet and outlet of the MHD power generation channel, we need to measure the static pressure and total pressure of the inlet and outlet of the channel. We define the inlet of the channel as cross section 1, and the outlet of the channel as cross section 2.

Cross section 1

$$p_{01} = p_1\left(1+\frac{\gamma-1}{2}Ma_1^2\right)^{\frac{\gamma}{\gamma-1}} \tag{26}$$

We assume the flow is isentropic, then, total pressure p_{01} is equal to p_e, p_1 is the inlet static pressure, subscript 1 indicates cross section 1.

And,

$$T_{01} = T_1\left(1+\frac{\gamma-1}{2}Ma_1^2\right) \tag{27}$$

For the shock tunnel, total temperature T_{01} is equal to T_e. And the inlet temperature T_1, Ma_1 can be obtained with Eqs. (26)-(27).

Application of the first law of thermodynamics to the MHD generator yields an energy balance in the form

$$m_a h_{02} = m_a h_{01}(1-\eta_{N(g)}) \tag{28}$$

where h_{01} and h_{02} are total enthalpy of cross section 1 and cross section 2, subscript 2 indicates cross section 2. From the fact that the flow is adiabatic in the channel, h_{02}= h_{01}, we can obtain

$$\frac{T_{02}}{T_{01}} = \frac{h_{02}}{h_{01}} = 1-\eta_{N(g)} \tag{29}$$

From Eq. (27) and Eq. (29), it can be found that

$$T_2\left(1+\frac{\gamma-1}{2}Ma_2^2\right) = T_1\left(1+\frac{\gamma-1}{2}Ma_1^2\right)(1-\eta_{N(g)}) \tag{30}$$

Cross section 2

$$p_{02} = p_2\left(1+\frac{\gamma-1}{2}Ma_2^2\right)^{\frac{\gamma}{\gamma-1}} \tag{31}$$

where p_{02} is the total pressure of MHD power generation channel, and p_2 static pressure of the outlet of the channel. Using Eqs. (30)-(31), we can obtain the outlet temperature T_2 and Ma_2. Then, the gas state parameters of inlet and outlet of the MHD power generation channel can be obtained through measuring additional three parameters p_1, p_2 and p_{02}.

4. Conclusions

(1) Under the conditions of nozzle inlet total pressure 0.32 MPa, total temperature 6 504 K, magnetic field strength about 0.5 T and nozzle outlet velocity 1 959 m/s, induction voltage and short-circuit current of the segmentation MHD power generation channel are measured, and the voltages acquired are identical with the theoretical calculation.

(2) The short-circuit current measured from electrode #6 is about 1 A. Due to the performance decline caused by electrode oxidation，the measured current is smaller than the real current.

(3) The conductivity calculated from the voltage and current is about 20 S/m. Under the conditions as presented in this paper, the maximum power density can rise up to 4.797 1 MW/m^3 when the load factor is 0.5, the enthalpy extraction rate is 0.34%, and the Hall parameter for electron is 0.308 6.

(4) Owing to the low magnetic field strength created by permanent magnet, MHD generation can hardly change the parameters of flow after the working section, so it is hardly possible to analyze them through experimental measurement. Finally, the principle and method of indirect testing for gas state parameters T_1, Ma_1, T_2 and Ma_2 are analyzed and proved.

References

[1] Kuranov A L, Korabelnicov A V, Kuchinskiy V V, et al. Fundamental techniques of the “AJAX” concept: modern state of research. AIAA-2001-1915, 2001.

[2] Gurijanov E P, Harsha P T. AJAX: new directions in hypersonic technology. AIAA-1996-4609, 1996.

[3] Li Y H, Li Y W, Su C B. Hypersonic engine of magnetohydrodynamic (MHD) combined with turbine and preliminary experimental investigation. The 2nd Hypersonic Science and Technology Conference. 2009. [in Chinese]

[4] Su C B, Li Y H, Chen B Q, et al. Experimental investigation of MHD flow control for the oblique shock wave around the ramp in low-temperature supersonic flow. Chinese Journal of Aeronautics 2010; 22(1): 22-32.

[5] Wang J, Li Y H, Chen B Q, et al. Experimental investigation on shock wave control by plasma aerodynamic actuation. Acta Aeronautica et Astronautica Sinica 2009; 30(8): 1374-1379. [in Chinese]

[6] Kuranov A L, Sheikin E G. MHD control on hypersonic aircraft under “AJAX” concept possibilities of MHD generator. AIAA-2002-490, 2002.

[7] Liu J H, Tong J Z, Xing J B, et al. Development survey of foreign scramjet with MHD energy bypass—a new high speed scramjet. Winged Missle 2003; 9: 45-46. [in Chinese]

[8] Yu D R, Tang J F, Bao W. MHD-arc-ramjet combined cycle for hypersonic propulsion. Acta Aeronautica et Astronautica Sinica 2007; 28(4): 769-775. [in Chinese]

[9] Isaiah M B, Schneider S. Hypersonic engine using MHD energy bypass with a conventional turbojet. AIAA-2003-6922, 2003.

[10] Adamovich I V, Rich J W, Schneider S J, et al. Magnetogasdynamic power extraction and flow conditioning for a gas turbine. AIAA-2003-4289, 2003.

[11] Bityurin V A, Lineberry J T, Litchford R J, et al. Thermodynamic analysis of the AJAX propulsion concept. AIAA-2000-0445, 2000.

[12] Kaminaga S, Tomioka S, Yamasaki H. Feasibility study on MHD energy bypass scramjet engine. AIAA-

2005-3226, 2005.
[13] Benyo T L. The effect of MHD energy bypass on specific thrust for a supersonic turbojet. AIAA-2010-0232, 2010.
[14] Lineberry J T, Begg L L, Castro J H, et al. HVEPS scramjet-driven MHD power demonstration test results. AIAA-2007-3880, 2007.
[15] Moeller T, Rhodes R, Lineberry J T, et al. HVEPS combustion driven MHD power demonstration tests. AIAA-2008-4097, 2008.
[16] Murray R C, Zaidi S H, Carraro M R, et al. Magnetohydrodynamic power generation using externally ionized, cold, supersonic air as working fluid. AIAA Journal 2006; 44(1): 119-127.
[17] Lee C H, Lu H Y. Quasi-one-dimensional parametric study for MHD generator in MHD bypass scramjet system. AIAA-2007-0644, 2007.
[18] Lu H Y, Lee C H, Dong H T. Characteristic of three dimensional supersonic MHD generator. Science in China Series G: Physics, Mechanics and Astronomy 2009; 52(4): 534-545. [in Chinese]
[19] Ju C X, Lu Y C, Jing B H. Open cycle MHD power generation. Beijing: Beijing Industry University Press, 1998. [in Chinese]

Biographies:

LI Yiwen Born in 1983, he is a Ph.D. candidate in Air Force Engineering University. His main research interest is hypersonic vehicle MHD technique.
E-mail: lee_yiwen@163.com

LI Yinghong Born in 1963, he received B.S. and M.S. degrees from Air Force Engineering University and Nanjing University of Science and Technology in 1983 and 1987 respectively. Now he is a professor in Air Force Engineering University. His main research interests include plasma dynamic, aeroengine fault diagnosis, reliability analysis.
E-mail: yinghong_li@126.com

LU Haoyu Born in 1978, he received Ph.D. degree from Beihang University in 2008. Now he is a lecturer in School of Astronautics, Beihang University. His main research interest is aeronautic and astronautic magnetohydrodynamics, especially numerical investigation.

ZHU Tao Born in 1987, he is now a graduate student in Air Force Engineering University. His main research interests are aeronautic magnetohydrodynamics and plasmadynamics.